Released carbonaceous exudates influence carbon sequestration in two ways: (i) partially breaking the crystalline structure to form SRO minerals having high carbon sequestering potential and (ii) acting as a source of carbon. From the present study, the following important conclusions can be drawn: (a) Carbon sequestration is a function of soil mineralogical constituents. It is governed not only by SRO aluminosilicates present in the soil, but also short-ranged iron and aluminium oxides and oxyhydroxides. (b) Fine clay humus in soil is most vital in terms of total amount of sequestered carbon, as higher amount of all the forms are being associated with that fraction. (c) In coarse clay humus fraction, role of Al and Fe compounds is more prominent. (d) Alfisol is the most potential soil for sequestering carbon than Vertisol and Inceptisol, and rhizosphere sequestered more carbon than non-rhizosphere.

1. Kumar, R., Pandey, S. and Pandey, A., Plant roots and carbon sequestration. *Curr. Sci*., 2006, **91**, 885–890.
2. Kuzyakov, Y. and Domanski, G., Carbon input by plants into the soil. *J. Plant Nutr. Soil Sci*., 2000, **163**, 421–431; doi: 10.1002/1522-2624(200008).
3. Vacca, S. *et al.*, From andic non-allophanic to non-andic allophanic Inceptisols on alkaline basalt in Mediterranean climate: a toposequence study in the Marghine district (Sardinia, Italy). *Geoderma*, 2009, **151**, 157–167; doi: 10.1016/j.geoderma.2009.03.024.
4. Chevallier, T., Woignier, T., Toucet, J., Blanchart, E. and Dieudonne, P., Fractal structure in natural gels: effect on carbon sequestration in volcanic soils. *J. Sol–Gel Sci. Technol*., 2008, **48**, 231–238; doi: 10.1007/s10971-008-1795-z.
5. Basile-Doelsch, I. *et al.*, Mineralogical control of organic carbon dynamics in a volcanic ash soil on La Réunion. *Eur. J. Soil Sci*., 2005, **56**, 689–703; doi: 10.1111/j.1365-2389.2005.00703.x.
6. Schnitzer, M., Humic substances: chemistry and reactions. In *Soil Organic Matter* (eds Schnitzer, M. and Khan, S. U.), Elsevier Publishing Co, Amsterdam, pp. l–64.
7. Egli, M., Nater, M., Mirabella, A., Raimondi, S., Plötz, M. and Alioth, L., Clay minerals, oxyhydroxide formation, element leaching and humus development in volcanic soils. *Geoderma*, 2008, **143**, 101–114; doi: 10.1016/j.geoderma.2007.10.020.
8. Tonneijck, F., Jansen, B., Nierop, L., Verstraten, K. and Sevink, J., Towards understanding of carbon stabilisation mechanisms in volcanic ash soils in Andean ecosystems. In IOP Conference Series: Earth and Environmental Science 6, 2009, 042033; doi: 10.1088/1755-1307/6/4/042033.
9. Christensen, B. T., Physical fractionation of soil organic matter in primary particle size and density separates. *Adv. Soil Sci*., 1992, **20**, 1–90.
10. Schollenberger, C. J., A rapid approximate method for determining soil organic matter. *Soil Sci.*, 1927, **24**, 65–68.
11. Blair, G. J., Lefroy, R. D. B. and Lisle, L., Soil carbon fractions based on their degree of oxidation, and the development of a carbon management index for agricultural systems. *Aust. J. Agricul. Res*., 1995, **46**, 1459–1466; doi: 10.1071/AR9951459.
12. Kramer, M. G., Sanderman, J., Chadwick, O., Chorover, J. and Vitousek, P., Long-term carbon stabilization through sorption of dissolved aromatic acids to reactive particles. American Geophysical Union, Fall Meeting, 2010, Abstract B31I-01.
13. Yuan, G., Theng, B. K. G., Parfitt, R. L. and Percival, H. J., Interactions of allophane with humic acid and cations. *Eur. J. Soil Sci*., 2000, **51**, 35–41; doi: 10.1046/j.1365-2389.2000.00295.x.
14. Manjaiah, K. M., Kumar, S., Sachdev, M. S., Sachdev, P. and Datta, S. C., Study of clay–organic complexes. *Curr. Sci*., 2010, **98**, 915–921.
15. Kothawala, D. N., Moore, T. R. and Hendershot, W. H., Soil properties controlling the adsorption of dissolved organic carbon to mineral soils. *Soil Sci. Soc. Am. J*., 2009, **73**, 1831–1842; doi: 10.2136/sssaj2008.0254.
16. Rasmussen, C., Torn, M. S. and Southard, R. J., Mineral assemblage and aggregates control carbon dynamic in a California conifer forest. *Soil Sci. Soc. Am. J*., 2005, **69**, 1711–1721; doi: 10.2136/sssaj2005.0040.
17. Woignier, T., Pochet, G., Doumenc, H., Dieudonné, P. and Duffours, L., Allophane: a natural gel in volcanic soils with interesting environmental properties. *J. Sol–Gel Sci. Technol*., 2007, **41**, 25–30; doi: 10.1007/s10971-006-7593-6.
18. Jones, D. L. and Edwards, A. C., Influence of sorption on the biological utilization of two simple carbon substrates. *Soil Biol. Biochem*., 1998, **30**, 1895–1902; doi: 10.1016/S0038-0717(98)00060-1.

Received 1 March 2013; revised accepted 18 September 2013

Electrical resistivity tomography for groundwater exploration in a granitic terrain in NGRI campus

S. N. Rai[1,*], S. Thiagarajan[1], Dewashish Kumar[1], K. M. Dubey[2], P. K. Rai[2], A. Ramachandran[3] and B. Nithya[3]

[1]CSIR-National Geophysical Research Institute, Uppal Road, Hyderabad 500 007, India
[2]Banaras Hindu University, Pandit Madan Mohan Malaviya Road, Varanasi 221 005, India
[3]Anna University, Chennai 600 025, India

Rapid growth of residential colonies around the campus of the CSIR-National Geophysical research Institute (NGRI), Hyderabad during the last two decades has resulted in either disappearance or drastic reduction in size of open space and ponds for groundwater recharging. Withdrawal of groundwater for domestic uses has increased several fold causing continuous lowering of the water table in and around the campus. Due to this changed scenario, availability of groundwater to meet the requirement of CSIR-NGRI is drastically reduced. This communication presents the results of electrical resistivity tomography (ERT) carried out in the CSIR-NGRI premises to locate potential groundwater resources as well as choose suitable sites for artificial recharging of aquifer. Groundwater potential zone identified by ERT is verified at one site by drilling a bore well.

Keywords: Artificial recharging, granite, groundwater resources, electrical resistivity tomography.

*For correspondence. (e-mail: snrai@ngri.res.in)

A MAJOR portion of water supply to meet the requirements of CSIR-National Geophysical Research Institute (NGRI) campus, Hyderabad is met from groundwater resources. Because of rapid growth of residential colonies and many-fold increase in the withdrawal of groundwater by the residents of colonies located around the CSIR-NGRI campus, the water table has been continuously declining. As a result dug wells and shallow bore wells within the campus and in the surrounding regions have dried up. This has resulted in acute shortage of water supply, especially during summer season. This situation has attracted the attention of the CSIR-NGRI authorities towards sustainable development and management of groundwater resources for safe and secure water supply to meet the water requirement of the campus. Geophysical electrical surveys with four electrode configuration such as Schlumberger, Wenner, dipole–dipole, pole–dipole are being widely used since more than five decades for delineation of groundwater resources in different geological provinces. For example, Bose and Ramkrishna[1] conducted electrical survey in parts of Sangli District, Maharashtra for delineation of groundwater resources. Rao *et al.*[2] have carried out electrical survey in Deccan traps-covered region of Aurangabad district, Maharashtra. Rai *et al.*[3–5] have carried out electrical resistivity survey for delineation of deeper sources of groundwater in parts of Katol and Kaleshwar taluks of Nagpur district, Maharashtra. In all these studies mostly vertical electrical sounding (VES) technique has been used. The greatest limitation of such a survey with four electrode configuration is that it provides only 1D model of resistivity variation below the centre of the survey profile and does not take into account lateral changes in the resistivity value on either sides of the centre due to the presence of geological formation/structure such as faults, fractures, joint, etc. which are the major sources of groundwater in hard-rock formations. Therefore, their delineation by 1D model is not always possible unless these structures coincidently lie below the centre of the profile. A more accurate model of the subsurface would be a 2D model which provides information about the resistivity variations in the vertical as well as lateral direction along the survey line.

Development of 2D resistivity models becomes possible with the development of electrical resistivity tomography (ERT) technique, which is also known as electrical resistivity imaging[6]. ERT is used worldwide for delineation of groundwater resources in complex hydrogeological set-up. The ERT survey was carried out over meta-sedimentary and metavolcanic terrains in the Harare greenstone belt in northeastern Zimbabwe as part of a groundwater resources investigation[7]. As part of the groundwater exploration programmes, ERT was applied to map the thickness of aquifer and bedrock in Banting, Selangor, Malaysia[8]. ERT was carried out at the periphery of the farm dam impounding reservoir of the Ahmadu Bello University in northern Nigeria, to study the subsurface seepage conditions and identify possible weak zone that could serve as seepage paths in the subsurface close to the dam[9]. ERT survey was used to delineate fractures at a solid waste disposal site in Unguwan Dosa, Kaduna State, Nigeria that may provide pathways for groundwater flow and contaminant transport[10]. To decipher groundwater potential zones for irrigation and drinking water purposes, ERT were carried out in Pagoh, and Johor, Malaysia[11], and in parts of Kubanni River Basin, Zaria, Nigeria[12]. Dutta *et al.*[13] have carried out ERT for delineation of groundwater resources in granitic terrain of Maheshwaram watershed in Ranga Reddy district, Andhra Pradesh. ERT has been carried out in the Chiplun taluk, Ratnagiri district, Maharashtra to delineate aquifers for exploration of groundwater and geothermal fluids[14]. Ratnakumari *et al.*[15] have carried out ERT for delineation of deeper aquifers in Deccan traps occupied Chandrabhaga river basin in Nagpur district. The present work deals with ERT carried out within the CSIR-NGRI campus to delineate potential groundwater resources to cope up with the ever-increasing demand for water supply.

The CSIR-NGRI campus located between 78°32′49.2″E to 78°33′25.2″E long. and 17°24′28.8″N to 17°25′8.4″N lat. in Hyderabad city, India, is spread over an area of ~150 acres (Figure 1). Uppal road lies to its SE, while IICT residential campus is on the western side and Kalyanpuri is located towards north-east direction of the campus. The campus area is covered by soil of varying thickness which is underlain by granite. Exposures of granite can be seen at many places in the campus. Groundwater in such geological environment occurs in the weathered mantle above the granitic formation and in faults and fracture zones within the granites. Delineation of such water-bearing geological formations/structures with more accuracy is possible with 2D resistivity modelling using ERT.

ERT is carried out using multi-electrode resistivity imaging system and effective data processing software based on inversion techniques. For ERT, multi-core cables with many electrode takeouts are connected together to form a multi-electrode set-up, where selection of any four (two for current injection and two for potential measurement) of those electrodes is possible. The number of electrodes differs from system to system. Some systems carry 64 electrodes, some carry 72 electrodes and so on. ERT equipment has been developed by a number of international companies. In the present study, the ABEM-made Terrameter LUND Imaging System, SAS 4000 resistivity meter is used. ERT is carried out using four multi-core cables each having 16 electrodes. Spacing between two electrodes is 10 m. Spread length for this ERT unit is 630 m. Spacing between electrodes can be reduced according to the requirements.

Figure 2 shows field arrangement of an ERT survey with four multi-core cables each fitted with 16 electrodes placed at equal distance. Selection of spacing between

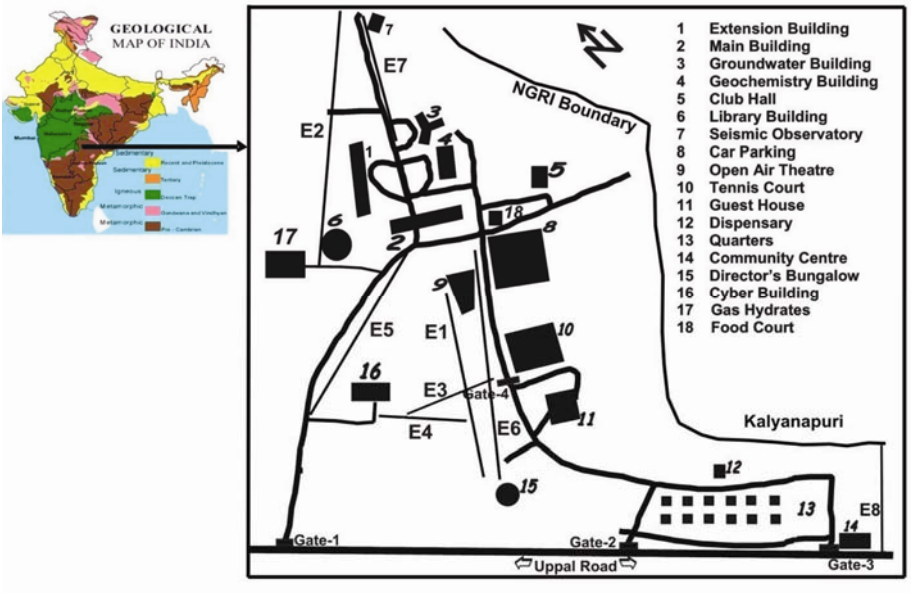

Figure 1. Layout map of CSIR-NGRI campus (not to the scale); location of electrical resistivity tomography (ERT) profiles are marked by E1–E8.

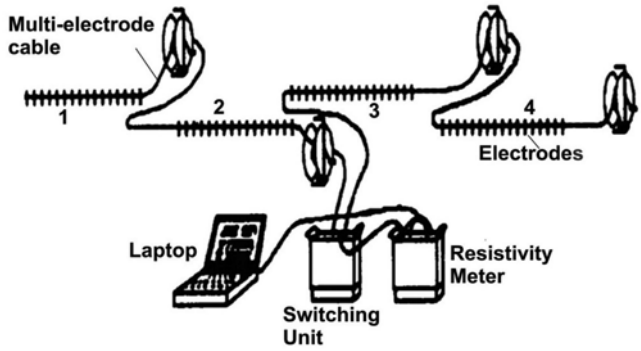

Figure 2. Field layout of ERT survey with four multi-core cables each fitted with 16 electrodes.

electrodes can be made based on the nature of survey. For subsurface images of high resolution, smaller spacing is used. Multi-core cables are connected to an electronic switching unit. This unit is connected to a resistivity meter which is connected to a laptop. Information regarding the sequence of measurements, type of array used and other survey parameters such as the intensity of current are entered in a text file which can be read by a computer program loaded onto the laptop. After reading the control file, the computer program automatically selects the appropriate electrodes (two current electrodes and two potential electrodes) for each measurement. The measurements are taken automatically and stored in the laptop.

For demonstration purpose, sequence of measurements to build up a pseudo section using multi-core cables fitted with 16 electrodes is shown in Figure 3. In this example, the spacing between adjacent electrodes is considered as a for the first sequence of measurements. The first step is to make all the possible measurements for the Wenner array with an electrode spacing of a. For the first measurement, electrodes numbers 1, 2, 3 and 4 are used. Electrode 1 is used as the first current electrode C1, electrode 2 as the first potential electrode P1, electrode 3 as the second potential electrode P2 and electrode 4 as the second current electrode C2. For the second measurement, electrode numbers 2, 3, 4 and 5 are used for C1, P1, P2 and C2 respectively. This procedure is repeated until electrodes 13, 14, 15 and 16 are used for the last measurement with spacing of a. The total number of first sequence of measurements for spacing a will be 13. The apparent resistivity, ρ_a, for spacing a is computed using the following expression

$$\rho_a = 2\pi a \frac{\Delta V}{I},$$

where I is the induced current and ΔV the potential difference between potential electrodes. After completing the first sequence of measurements with spacing a, the second sequence of measurements with spacing $2a$ is made. Electrodes 1, 3, 5 and 7 are used for the first measurement. The electrodes are chosen so that the spacing between adjacent electrodes is $2a$. For the second measurement, electrodes 2, 4, 6 and 8 are used. This process is repeated until electrodes 10, 12, 14 and 16 are used for the last measurement with spacing $2a$. The same process is repeated for measurements with spacing $3a$, $4a$ and $5a$. For spacing $5a$ there is only one measurement. Thus, the total number of measurement is 35 for one-time laying of the multi-core cables containing 16 electrodes, instead of only one measurement for a conventional survey with

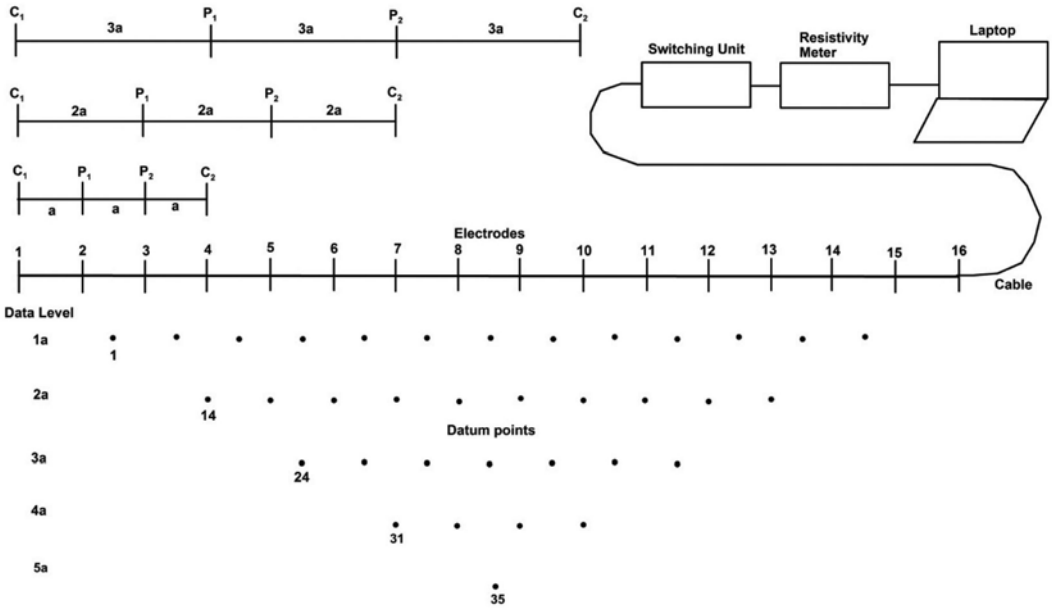

Figure 3. Sequence of measurements used to build a pseudo section.

four electrodes. As the electrode spacing increases, the number of measurements decreases.

It is evident from Figure 3 that the depth coverage by ERT is maximum below the central part of the profile and it decreases with distance away from the centre. To complete the depth coverage laterally, roll-along procedure of surveying is used. In this procedure, after completing the sequence of measurements for one field set-up, the cable is moved along the survey profile towards one of its ends by several units of electrode spacing in such a way that in the second sequence of measurements, the depth coverage remaining in the previous sequence of measurements is completed during the measurements made in the second sequence. Thus it is possible to achieve complete depth coverage of the resistivity measurements for a desired segment of the survey line. ERT can be carried out using different electrode arrays such as Wenner, Schlumberger, dipole–dipole, pole–dipole and pole–pole. Application of ERT for various purposes, including delineation of aquifer is described in detail by Loke[16].

The next step is to convert the measured apparent resistivity values to a 2D subsurface true resistivity model which can be used for geological interpretation in order to identify water-bearing geological formations and structures such as weathered mantle, fractures, faults, joints, etc. This task is accomplished using inverse modelling. Inverse modelling of the measured apparent resistivity data is carried out using RES2DINV program[17] to create a subsurface resistivity model. This program automatically creates a 2D model by dividing the subsurface into rectangular blocks. To initiate modelling work some resistivity values will be assigned to the model blocks. Thereafter, the program calculates the apparent resistivity values of the model blocks and compares them to measured apparent resistivity values. The resistivity value of the model block is adjusted iteratively until the calculated apparent resistivity values of the model are in close agreement with the measured apparent resistivity values. The final output is a 2D model of subsurface resistivity variations for different geological formations. The resistivity model also presents associated root mean square (RMS) error value, which is obtained by first calculating the residuals between the measured and calculated values of the resistivity. Squaring the residuals, averaging the squares and then taking the square root gives the RMS. If the value of the RMS error is preferably <10% or close to it, then it is considered as the realistic subsurface model for good quality data. In general, it is related to data quality. Geological interpretation of this resistivity model is used for identification of groundwater potential zones. The main advantages of 2D ERT over the conventional electrical survey by four-electrode array are: (1) automated acquisition of large amount of data in less time at lower cost, and (2) presentation of images of subsurface litho units along the entire survey line with high resolution.

In the present work, ERT is carried out at eight sites using Wenner configuration. Locations of ERT profiles are marked as E1–E8 in Figure 1. Details of profiles are given in Table 1. Inverse resistivity models for these profiles along with associated RMS values, resistivity value index, direction of profiles and spacing of electrodes are given in Figure 4. The next step is the interpretation of inverse resistivity model in terms of geological formation which helps in identification of groundwater potential zones. Hereafter, only resistivity model will be used for the inverse resistivity model.

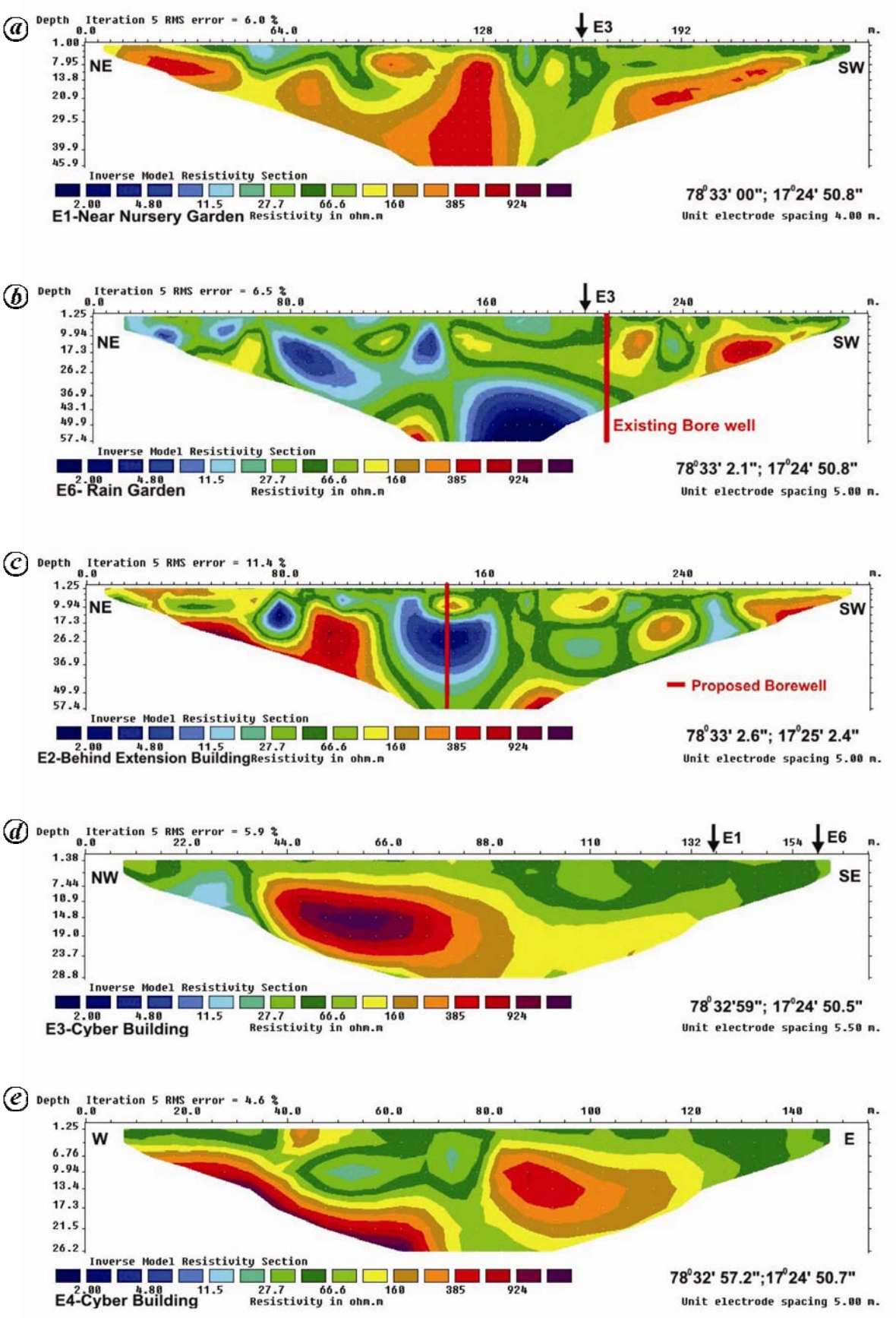

Figure 4. (*Contd…*)

(*Contd…*)

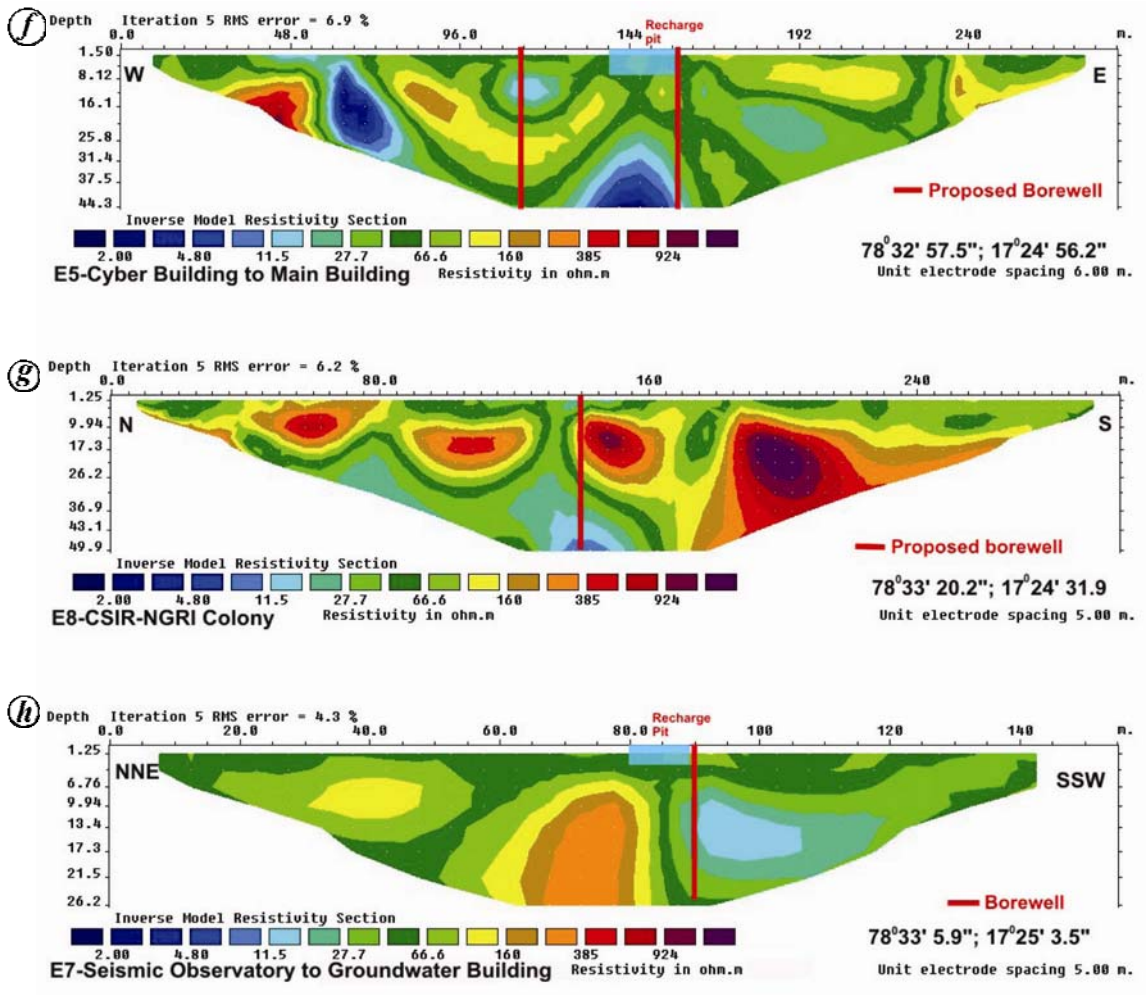

Figure 4. Resistivity models for different profiles. ***a***, E1; ***b***, E6; ***c***, E2; ***d***, E3; ***e***, E4; ***f***, E5; ***g***, E8; ***h***, E7.

Table 1. Resistivity values for different litho units[18]

Litho unit	Resistivity (Ohm m)
Soil cover	< 20
Highly weathered granite	20–50
Semi-weathered granite	50–120
Fractured/jointed granite	120–200
Massive granite	> 300

Table 2. Details of the profiles

Profile no.	Coordinates of the centre	Length of the profile (m)	Spacing between two electrodes (m)
E1	78°33′00″E; 17°24′50.8″N	252	4
E2	78°33′22.6″E; 17°25′2.4″N	315	5
E3	78°32′59″E; 17°24′50.5″N	160.5	5.5
E4	78°32′57.5″E; 17°24′50.7″N	145	5
E5	78°32′57.5″E; 17°24′56.2″N	282	6
E6	78°33′2.6″E; 17°25′2.4″N	315	5
E7	78°33′5.9″E; 17°25′3.5″N	155	5
E8	78°33′20.2″E; 17°24′31.9″N	300	5

Based on the resistivity surveys carried out in different granitic terrains, the Central Ground Water Board (CGWB), Ministry of Water Resources, Government of India has suggested the resistivity values of different litho units of granitic terrains[18]. Litho units and their corresponding resistivity values are given in Table 2. Our field experience suggests that the formations with resistivity values in the range 15–40 Ohm m represent good aquifers, 40–55 Ohm m represent moderate aquifers and >70 Ohm m represent massive granites. More or less the same values with some modifications are used to interpret the resistivity model.

Profile E1 is located between a point on the western side of the open-air theatre and another point close to the northern side of the Director's bungalow. The set-up of the profile and its resistivity model are shown in Figure 4 *a*. Markings by small vertical lines along profiles represent positions of the electrodes. Totally 64 electrodes are used for the survey. The number given with an associated electrode is the distance measured from the first electrode

whose position is marked with zero on the profile line. For example, 64 on the profile line is the distance of the 17th electrode measured in metres from the first electrode. Bar scale of resistivity values in the range 2–925 Ohm m is given immediately below the resistivity models. The same bar scale of the resistivity values is used for all models. It is evident from the figure that the geological formations for this profile are characterized with resistivity values close to or more than 70 Ohm m, indicating absence of promising groundwater zone suitable for exploitation. E3 at 156 m distance indicates the location where profile E3 crosses profile E1.

Profile E6 runs between a road that passes through gate number 4 and the eastern margins of the nine recharge pits located in a row. This profile is extended near to the northern boundary of the Director's bungalow. Resistivity model for this profile is presented in Figure 4 *b*. Marking of E3 at 200 m distance indicates the location where profile E3 crosses profile E6. Recharge pits 1–9 are located between 80 and 205 m in sequence from NE to SW. The resistivity model indicates presence of water-bearing aquifer zone characterized by resistivity values < 40 Ohm m between 150 and 200 m distances at ~30 m depth. Depths are measured from the ground surface. This aquifer zone is overlain by a massive granite unit and shows tendency of extension towards SE direction below the massive granite. Presently, a bore well located near gate no. 4 is being used for groundwater pumping from this aquifer. This bore well is 13 m away from the profile towards gate no. 4. Its projection on the profile is marked at 210 m distance. It confirms the potentiality of the water-bearing aquifer. Recharge pits 1–4 are positioned between 80 and 145 m and the remaining pits numbering 5–9 are positioned between 145 and 205 m. From the resistivity model it is evident that the recharge pits 1–4 are within the weathered/fractured granite (< 40 Ohm m), which is connected to the aquifer zone and are contributing towards its recharging. Presence of moist formation characterized by resistivity value < 20 Ohm m within the weathered/fractured granite unit (20–40 Ohm m) can be seen in the figure between 80 and 145 m. The weathered/fracture granite unit is underlain by a massive granite unit, which interfaces the water-bearing aquifer below 145 m. On the other hand, recharge pits 5–9 are positioned within moderately fractured granite (~40 Ohm m), which is underlain by massive granite unit. This unit prevents recharging of aquifer from the overlying recharge pits. Suitable site for bore well drilling on this profile is suggested at 160 m distance near to the contact zone with the massive granite.

Profile E2 runs almost in NE–SW direction from a point located near the CSIR-NGRI boundary opposite the Seismic observatory up to a road in front of Gas Hydrate building. Resistivity model of this profile indicates the presence of water-bearing fracture zone between 120 and 160 m distances. Its downward extension is mapped only up to 57.4 m. A bore well is proposed at 145 m distance for groundwater exploitation.

Profile E3 extends from the corner of the eastern boundary wall of the Cyber building to near gate no. 4 through the forest area. Two low-resistivity zones characterized by resistivity value < 40 Ohm m are seen at both ends of the profile. The first low-resistivity zone exposed to the ground surface between 22 and 33 m distances near the northeastern edge of the profile is imaged only up to 15 m depth and appears to be extending beyond it. A small segment of the second low-resistivity zone exposed to the ground surface is visible near the southeastern edge of the profile. Profile E3 intersects profiles E1 and E6 at 137 and 159 m distances respectively. Intersection points are marked by E1 and E6 on profile E3. Geological formations at the intersection point of E3 on profile E1 and at the intersection point of E1 on profile E3 are found to be the same, characterized by resistivity values in the range 50–66 Ohm m. Similarly, geological formations at the intersection point of E3 on profile E6 and at the intersection point of E6 on profile E3 are found to be the same, characterized by resistivity value < 40 Ohm m. The investigated depth at the intersection point of E3 on E6 is ~3 m only because of its location near the end-point of the profile. Occurrence of the same geological formations at the respective intersection points confirms the compatibility of inverted resistivity sections of profiles E1, E6 and E3.

Profile E4 runs between a point near the road-crossing in front of the Cyber building and another point located behind the Director's bungalow. Resistivity model of this profile is presented in Figure 4 *e*. This figure presents a zone of low resistivity (< 40 Ohm m) formation below ~4 m thick cover of massive and fractured granite between 40 and 70 m. This low-resistivity zone is connected to a moderately fractured zone which separates two units of massive granite (<70 Ohm m). This could possibly be a water-bearing zone which needs to be verified by borewell drilling. Presence of geological formation of low-resistivity value (<40 Ohm m) is also indicated in the resistivity model towards the eastern end of the profile between 140 and 145 m distances. However, its depth extent beyond 10 m could not be mapped because of non-availability of space to extend the profile.

Profile E5 is located along the road connecting gate no. 1 to the main building. Resistivity model of this profile is presented in Figure 4 *f*. The model indicates exposure of a low-resistivity formation (<30 Ohm m) between 36 and 66 m. This formation is extending eastwards and its extension is again seen with the highest peak below the centre of the profile at 144 m. This zone appears to be suitable for groundwater exploitation. Two suitable alternative locations for bore-well drilling at 114 and 156 m distances are indicated in the figure. A site suitable for artificial recharging of the aquifer is proposed between 36 and 66 m.

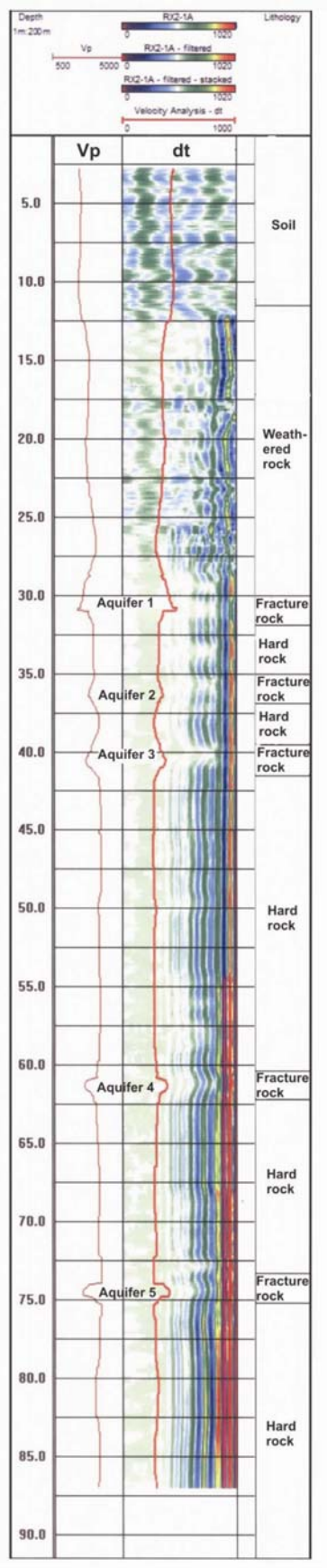

Figure 5. Sonic log for bore well at profile E7.

Profile E8 runs between boundaries adjacent to Uppal Road and Kalyanpuri colony. Resistivity model for this profile is presented in Figure 4 *g*. Resistivity model indicates the presence of massive granite along the entire profile length on the top. This massive granite layer is underlain by a low-resistivity formation (< 40 Ohm m) between 40 and 160 m distance, which is the centre of the profile. This could be a groundwater potential zone favourable for groundwater exploitation. Depth of this water-bearing zone increases with distance up to the centre of the profile. Thereafter, its lateral extension towards south is blocked by massive granite. This water-bearing zone is connected to a 5 m wide fracture zone which is exposed on the ground surface between 130 and 135 m. At this location a recharge pit or injection well is proposed to divert rain water collected from rooftops of the nearby quarters and run-off into the aquifer for recharging. Location of a bore well is proposed at 140 m distance near the contact zone of the water-bearing formation with the massive granite unit.

Profile E7 is located along the road connecting the Seismological observatory to the Groundwater building. Resistivity model for the profile is given in Figure 4 *h*. A contact zone between a massive granite unit and low-resistivity formations (< 40 Ohm m) consisting of soil on the top and water-saturated weathered/fractured formations at the bottom is seen up to a depth of 26 m towards SSW direction beyond 85 m distance. This low-resistivity geological formation appears to be extending further downwards and is a potential source of groundwater. In order to verify the interpreted litho units of this site, a bore well is drilled up to a depth of 100 m at 90 m distance, as shown in the Figure 4 *h*. Selection of the site for bore-well drilling is based on two criteria. First is the occurrence of maximum thickness of the water-bearing low-resistivity formation near the contact zone. Presence of massive granite facing water bearing formation will restrict lateral movement of groundwater beyond the interface. It will lead to the storage of groundwater in the contact zone in the entire thickness of the aquifer. The second criterion is the slope of the base of water-bearing formation towards the contact zone, which also facilitates accumulation of groundwater in the contact zone. Groundwater collected in the contact zone may have possibility of percolation into deeper aquifers in case of their connectivity with the contact zone. Sonic (or acoustic) logging was carried out in the bore well. The sonic log presents travel time of an elastic wave through the geological formations. This information is used to derive the velocity of elastic waves through the formation. Both information help in the identification of water-bearing geological formations and structures such as faults, fractures, etc. Results of sonic log in the form of elastic wave (V_p) and travel time (dt) are presented in Figure 5. In water-saturated fractures, an increase in the travel time will be seen which will cause a corresponding decrease in

V_p. Results of sonic log confirm the presence of water-saturated weathered formation beyond 20 m depth, which is connected to a water-saturated fractured zone marked as aquifer 1 at ~33 m depth. This leads to the raising of water level in the bore well up to a depth of 10.70 m below the ground surface. The other water-saturated fractures marked as aquifers 2, 3, 4 and 5 are identified at 37, 41, 62 and 74 m depths respectively. Sonic log up to a depth of ~13 m is erroneous and may be due to sealed casing. Groundwater yielding capacity of the bore well was tested by pumping continuously for 6 h a day for two days using 2HP motor. The yield of the bore well is 1.5 l/s, which is considered very good. A recharge pit between 85 and 100 m is suggested to divert the surface run-off into subsurface to sustain the availability of groundwater. The bore well is presently being used for water supply.

ERT along eight profiles is carried out in the granitic terrain of CSIR-NGRI campus to delineate groundwater potential zones in order to meet its ever-increasing demand for water supply. Four sites suitable for drilling bore wells and three sites suitable for managing artificial recharge are suggested. Locations of the suggested bore-well sites are shown in the resistivity models for profiles E2, E5, E7 and E8. Occurrence of groundwater potential zone related to profile E6 is verified by an existing bore well located near gate no. 4. Similarly, occurrence of groundwater potential zone related to profile E7 is verified by drilling a new bore well. A new site of bore well at 160 m on profile E6 is also suggested. Comparison of resistivity models of Figure 4 *g* and *h* indicates similarity in the subsurface geological set-up in terms of presence of contact zones between water-bearing zones and massive granite units. This indicates that the chance of occurrence of potential groundwater zone for profile E8 is as good as in case of profile E7. Three recharge sites are suggested at suitable locations on profiles E5, E7 and E8. Artificial recharging is already in practice for profile E6 through recharge pits 1–4. Groundwater exploration and managing aquifer recharging from suggested sites may help in safe and secured water supply to meet the ever-increasing demand of the CSIR-NGRI campus. In conclusion, ERT is a useful method for accurate mapping of groundwater potential zones, especially in complex hydrogelogical environs of hard-rock terrains where geological formations/structures vary drastically within a few metres, as shown in the resistivity models. The present work may serve as role model for groundwater exploration in other parts of the granitic terrains using ERT.

1. Bose, R. N. and Ramkrishna, T. S., Electrical resistivity surveys for ground water in the Deccan trap country of Sangli district, Maharashtra. *J. Hydrol*., 1978, **38**, 209–221.
2. Rao, T. G., Athavale, R. N., Singh, V. S., Muralidharan, D. and Murthy, N. N., Geophysical exploration for ground water in Deccan traps of Godavari–Purna basin, Maharashtra, NGRI Technical Report No. GH 18-GP10, 1983.
3. Rai, S. N., Thiagarajan, S. and Ratnakumari, Y., Exploration of groundwater in the basaltic Deccan traps terrain in Katol taluk, Nagpur district, India. *Curr. Sci.*, 2011, **101**(9), 1198–1205.
4. Rai, S. N., Thiagarajan, S., Ratnakumari, Y. and Kumar, D., Exploring Deccan traps for groundwater in parts of Kalmeshwar taluk, Nagpur district, India. *J. Appl. Hydrol*., 2012, **XXV**(3&4), 85–94.
5. Rai, S. N., Thiagarajan, S., Ratnakumari, Y., Anand Rao, V. and Manglik, A., Delineation of aquifers in basaltic hard rock terrain. *J. Earth Syst. Sci.*, 2013, **122**(1), 29–41.
6. Griffiths, D. H. and Barker, R. D., Two-dimensional resistivity imaging and modeling in areas of complex geology. *J. Appl. Geophys.*, 1993, **29**, 211–226.
7. Owen, R. J., Gwavava, O. and Gwaze, P., Multi-electrode resistivity survey for groundwater exploration in the Harare greenstone belt, Zimbabwe. *Hydrogeol. J*., 2005, **14**, 244–252.
8. Hamzah, U., Yaacup, R., Samsudin, A. R. and Ayub, M. S., Electrical imaging of the groundwater aquifer at Banting, Selangor, Malaysia. *Environ. Geol*., 2006, **49**, 1156–1162.
9. Osazuwa, I. B. and Chii, E. C., Two-dimensional electrical survey around the periphery of an artificial lake in the Precambrian basement complex of northern Nigeria. *Int. J. Phys. Sci.*, 2010, **5**(3), 238–245.
10. Abdullahi, N. K. and Osazuwa, I. B., Geophysical imaging of municipal solid waste contaminant pathways. *Environ. Earth Sci*., 2011, **62**, 1173–1181.
11. Kadri, Md. and Nawawi, M. N. M., Groundwater exploration using 2D resistivity imaging in Pagoh, Johor, Malaysia. In AIP Conference Proceedings, 2010, vol. 1325(1), pp. 151–154.
12. Anthony, A. A. and John, R. O., 2-D Electrical imaging and its application in groundwater exploration in part of Kubanni river basin, Zaria, Nigeria. *World Rural Obs.*, 2010, **2**(2), 72–82.
13. Dutta, S., Krishnamurthy, N. S., Arora, T., Rao, V. A., Ahmed, S. and Baltassat, J. M., Localization of water-bearing fractured zones in a hard rock area using integrated geophysical techniques in Andhra Pradesh. *Hydrogeol. J*., 2006, **14**, 760–766.
14. Kumar, D., Thiagarajan, S. and Rai, S. N., Deciphering geothermal resources in Deccan traps region using electrical resistivity tomography technique. *J. Geol. Soc. India*, 2011, **78**, 541–548.
15. Ratnakumari, Y., Rai, S. N., Thiagarajan, S. and Kumar, D., 2-D Electrical resistivity imaging for delineation of deeper aquifers in a part of the Chandrabhaga river basin, Nagpur district, Maharashtra, India. *Curr. Sci.*, 2012, **102**(1), 61–69.
16. Loke, M. H., Electrical imaging surveys for environmental and engineering studies – a practical guide to 2-D and 3-D surveys, 2000, p. 37.
17. Loke, M. H., Software: RES 2D INV. 2-D Interpretation for DC resistivity and IP for Windows 95. 1997, Copyright by M.H. Loke. 5, Cangkat Minden Lorong 6, Minden Heights, 11700 Penang, Malaysia.
18. CGWB website. Geophysical studies; http:/cgwb.gov.in/CR/achi_geo_stu.html

ACKNOWLEDGEMENTS. We thank Prof. Mrinal K. Sen, Director, CSIR-NGRI, Hyderabad for permission to publish this work, and Dr T. Seshunarayana for arranging well-logging.

Received 6 March 2013; revised accepted 4 September 2013